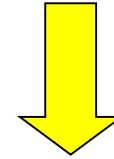


Micro-quasars

Binary systems with accretion onto compact object



Cataclysmic variables



White dwarf

X binaries



Neutron star

Black hole



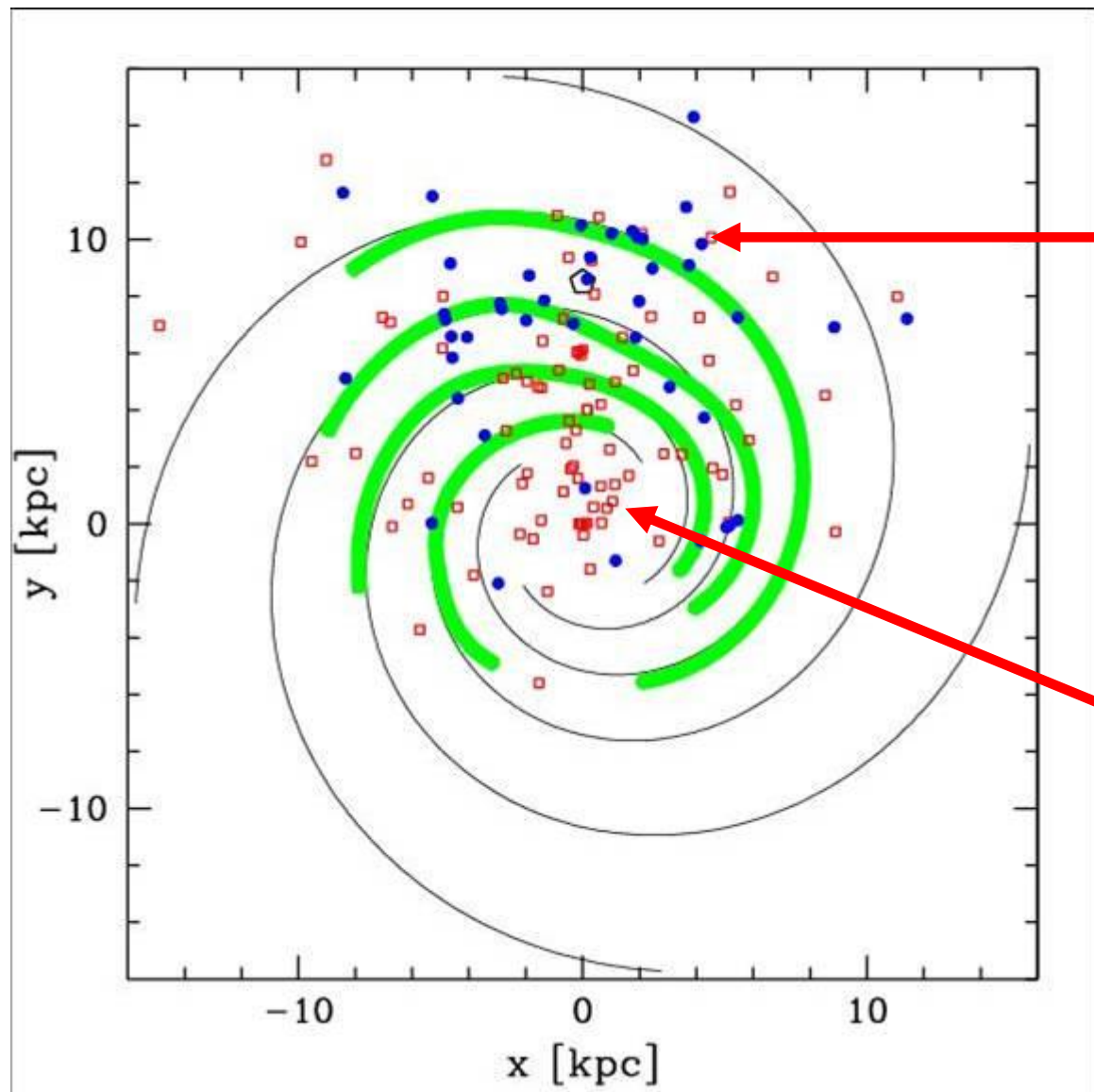
Classification based on the mass of the donor star:

➤ **LOW-MASS X-RAY BINARIES**

Old star (pop II): accretion through the Lagrangian point of the Roche lobe;

➤ **HIGH-MASS X-RAY BINARIES**

Young star (pop I): accretion through stellar wind



HMXRB

LMXRB

Micro-quasars: Galactic X-binaries with stellar BH (or NS) and relativistic jets

- Relativistic jets ($v > 0.1c$)
- Accretion disk onto compact object
- Strong source of non-thermal radiation
- Variability
- Physical and morphological properties similar to AGN , but much shorter time scale (f.e. observations on short time scale variability \rightarrow direct changes in the disk-jet system, inflow-outflow)

Properties of micro-QSO:

- ~ 200 X binaries => >15% have radio emission
- The first micro-QSOs detected at X and gamma frequencies
- 15 micro-QSOs have collimated jets with real velocities from 0.3c to 0.98c
- The typical energy is $\sim 10^{37}$ erg/s

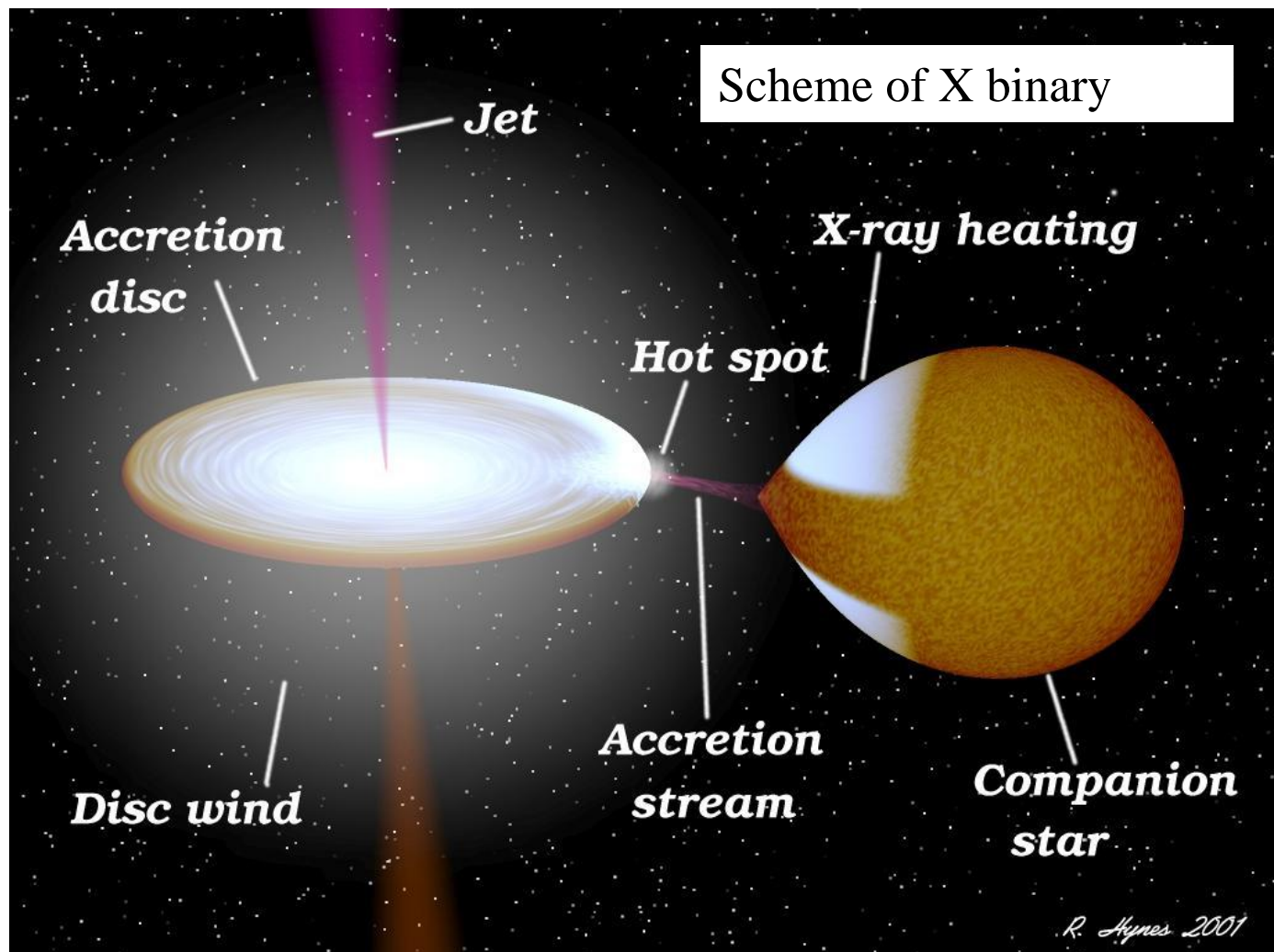
The first jets were observed in AGN then in the Galaxy

Rees (1984) showed that the characteristic temperature of a black body in the last stable orbit in the accretion disk is:

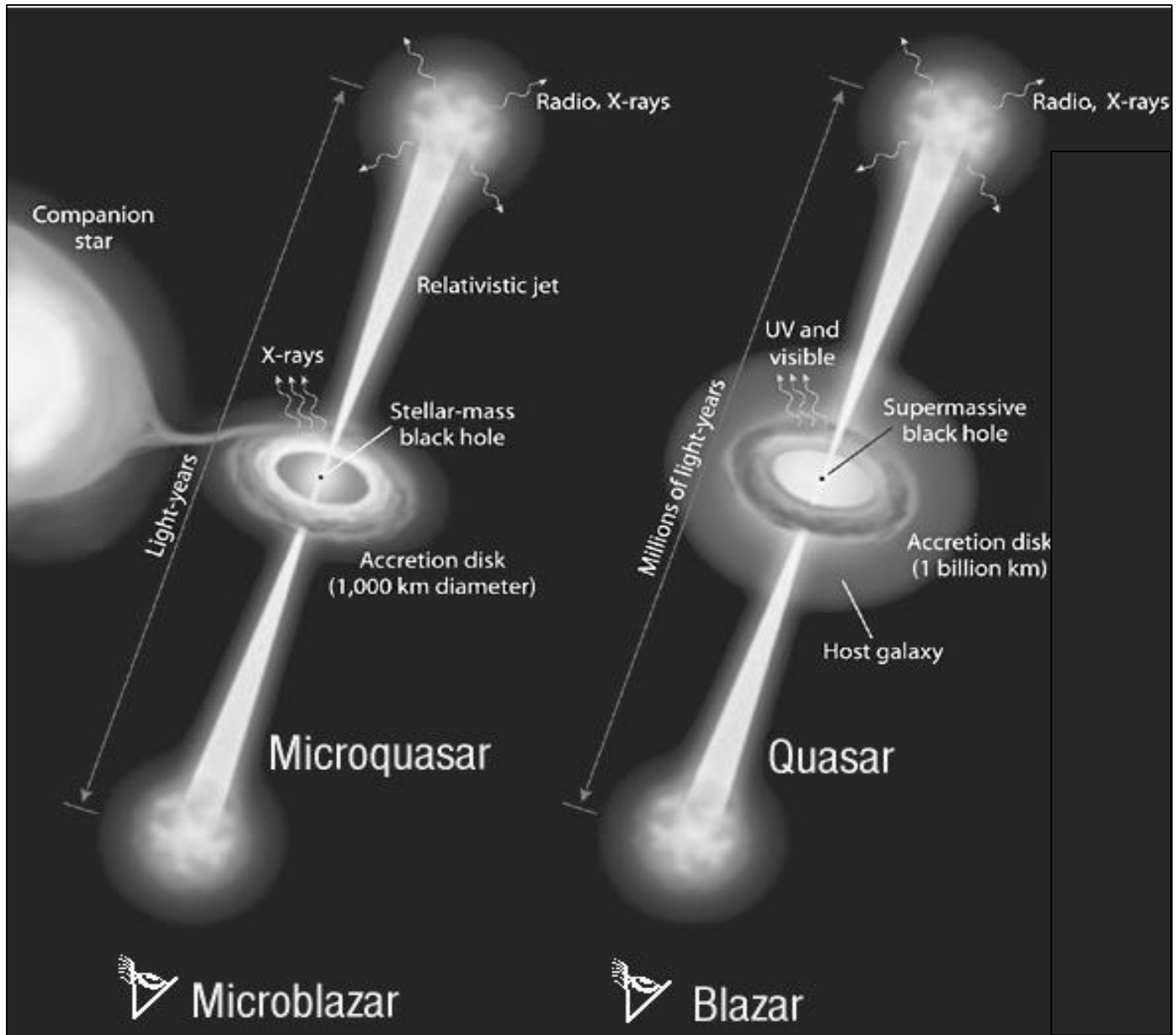
$$T \sim 2 \times 10^7 M^{-1/4} \quad (T, M \text{ of the black hole})$$

(the more massive is the BH the colder is the accretion disk around it
=> in AGN the emission is at visible and UV wavelengths, in the galactic sources the emission is at X and gamma wavelengths)

SS433. peculiar object, emits at optical frequencies.



black hole
accretion disk heated by the viscous dissipation
collimated jets of relativistic particles



MICROQUASARS



QUASARS

$$10^{37} \text{ erg / s}$$

Luminosity

$$10^{47} \text{ erg / s}$$

$$\sim 10^6 \text{ K}$$

accretion disk T

$$\sim 10^3 \text{ K}$$

$$10^{-9} M_{sol} / yr$$

Accretion rate

$$10 M_{sol} / yr$$

few l.y.

Jet length

$$10^6 \text{ l.y.}$$

$$1 - 10 M_{sol}$$

Black hole mass

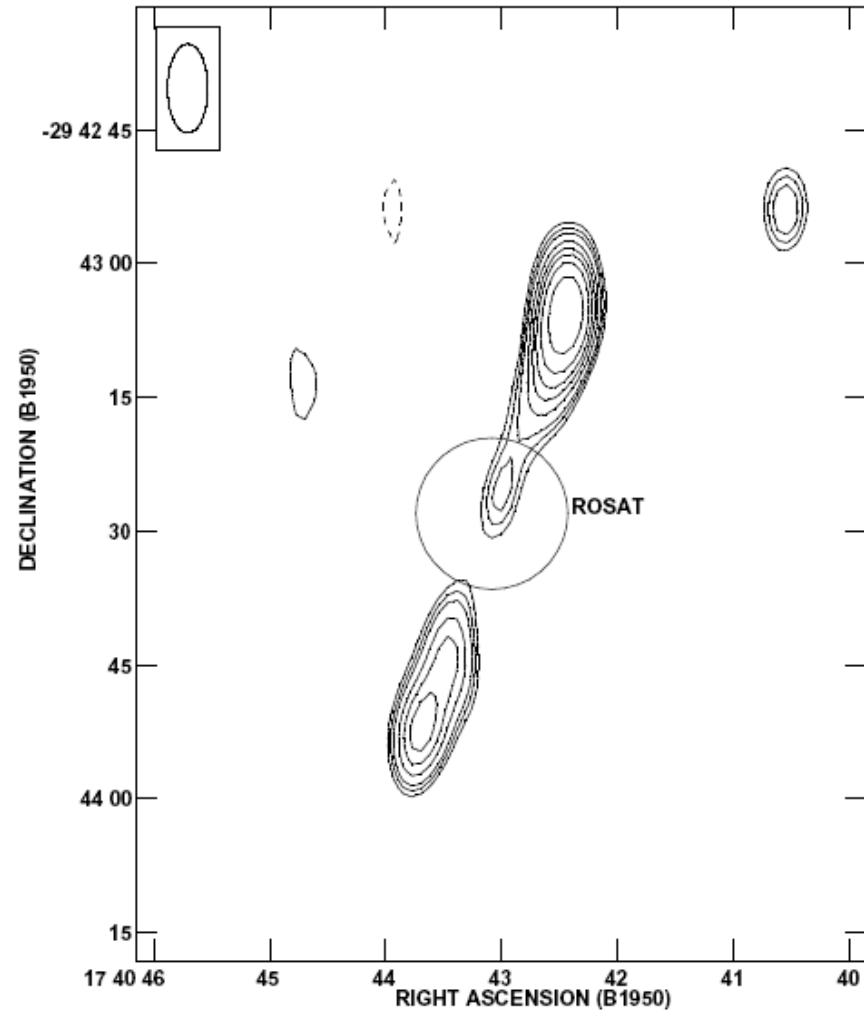
$$10^7 - 10^9 M_{sol}$$

Example: 1E1740.7-2942

Distance 8kpc

Jet ~5pc

It coincides with the Great Annihilation, which is the origin of a gamma-ray emission at 511 keV. The hypothesis is that the line is due to the annihilation of electrons-positrons.



Map at 6 cm (VLA, Mirabel+ (1992, 1999))

Circle: ROSAT position

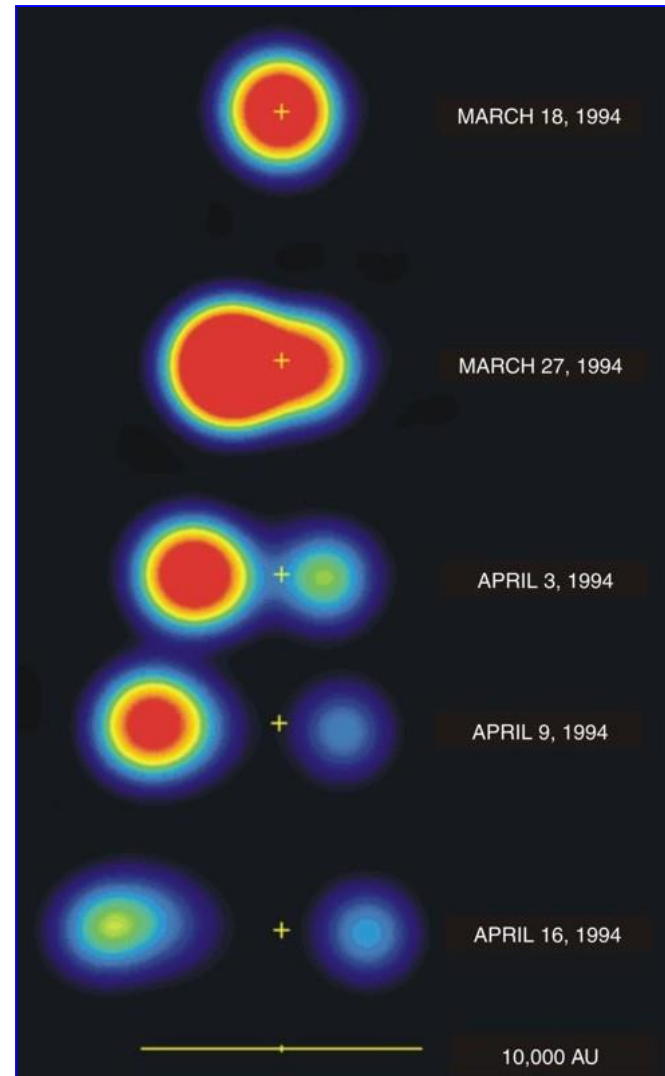
Example: GRS1915+105

- Discovered in 1994
- Star K-M + BH (d~12 kpc)
- Variable at various λ
- Hard X source
- Asymmetry in brightness due to relativistic Doppler boosting
- High accretion rate
- Superluminal motions (125% c)

$$v_{jet,true} \geq 0.9c$$

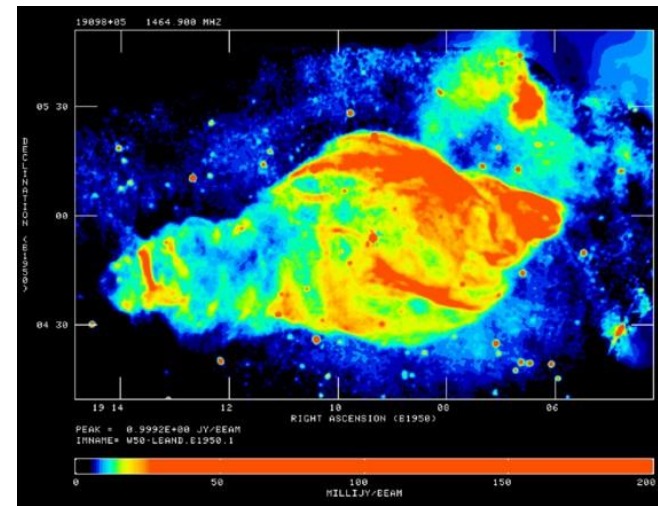
$$M_{BH} \approx 14M_{SUN}$$

(angle ~ 70deg. with line of sight)

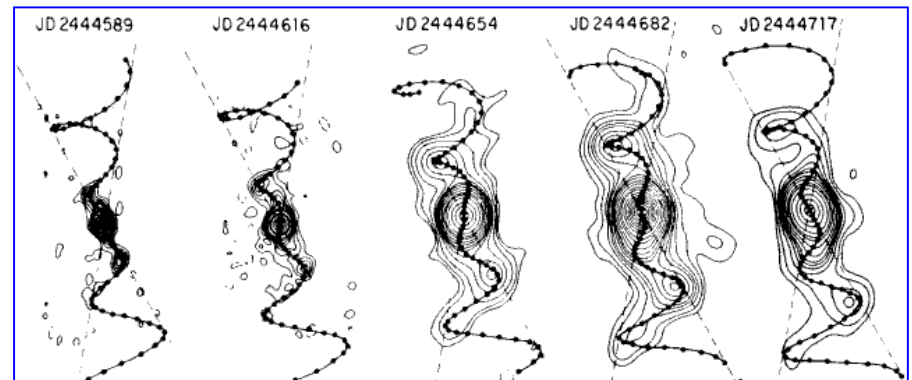
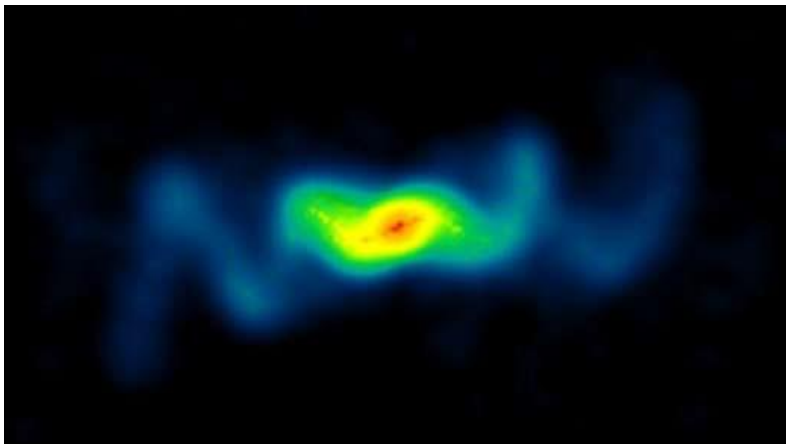


Example: ss433

- Discovered in 1984
- In W50 (SNR)
- Distance 5.5 ± 0.2 kpc
- Young star + BH
- Precession of the jets observed at X-ray and optical frequencies



SNR W50
In radio

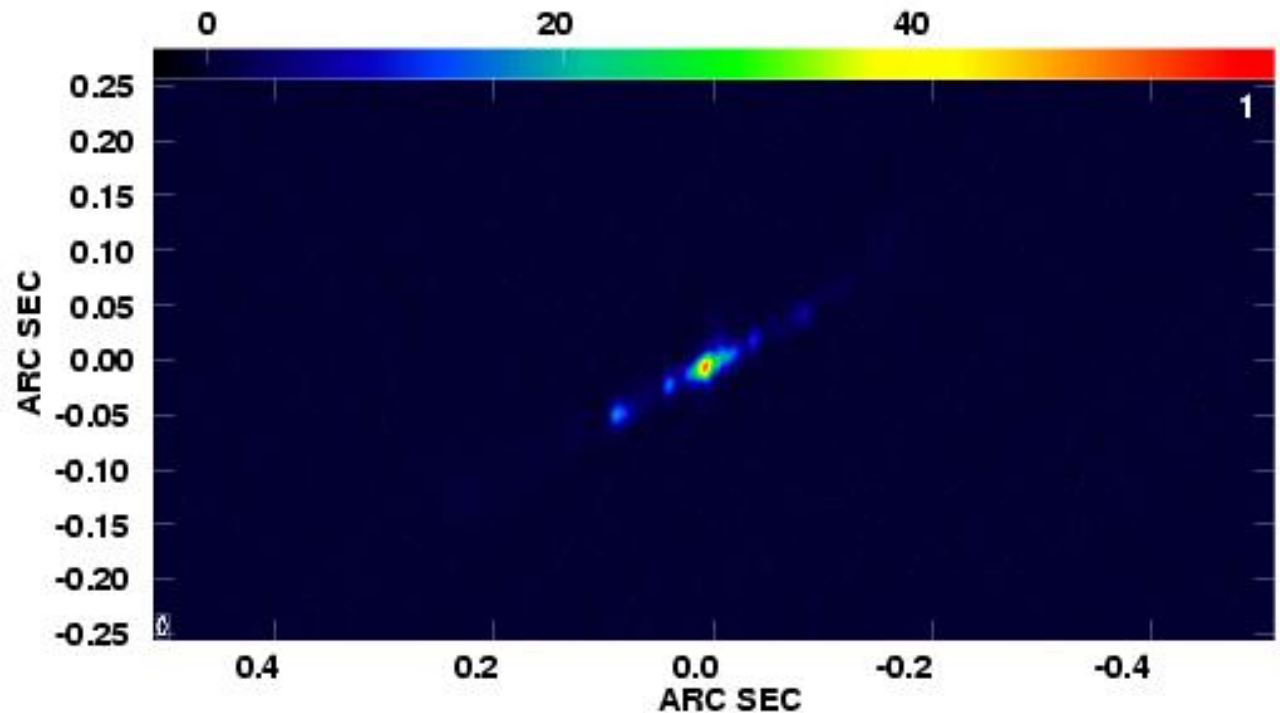


The radio image of the jets with the corkscrew shape

SS433

The jet precession is fitted with a kinematic model:

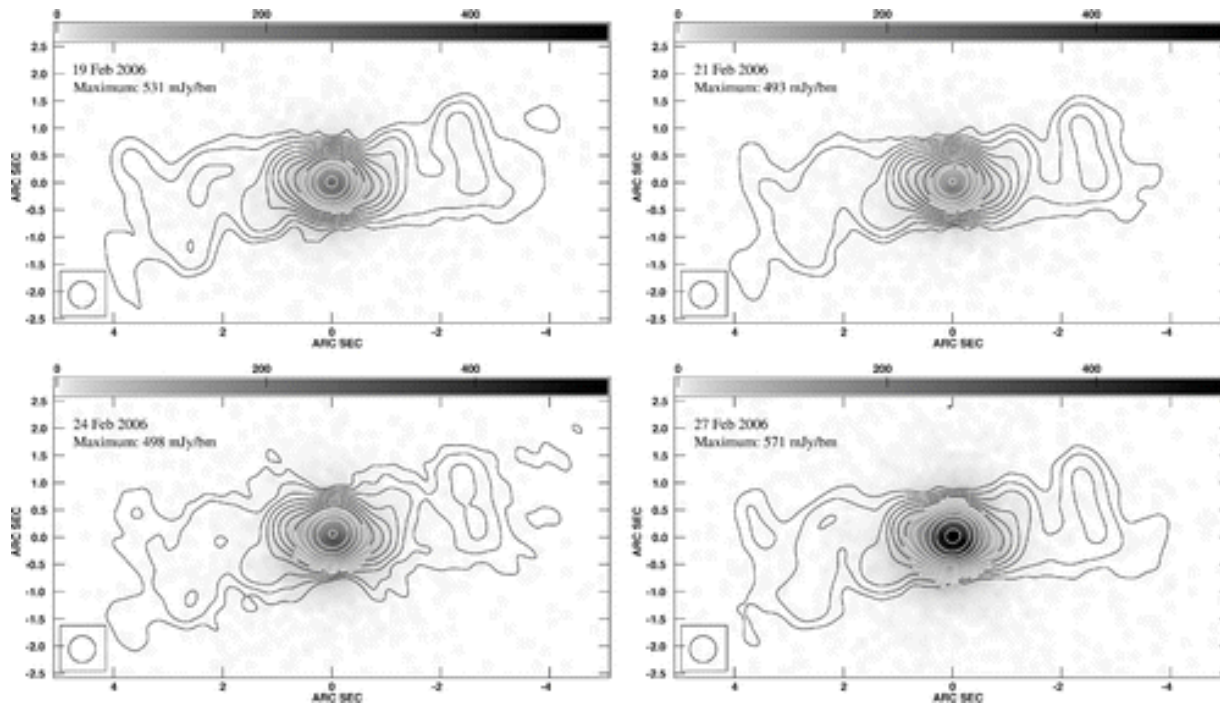
- Two collimated jets (20 deg.) which precess around an inclined (79 deg.) axis with respect to the line of sight, with a period of 164 d
- Velocity of the material in the jet $v_{jet} \approx 78 \times 10^3 \text{ km/s} \sim 0.26c$
- Asymmetry in the morphology of the jets (could be intrinsic)



SS433

Comparison radio (VLA) / X (Chandra) to study the relation between the two emission:

- The presence of the X-ray jets with arcsec scale is transient and there is no correlation with the radio flux density of the core
- The X-ray emission is not the tail of the synchrotron spectrum



Miller-Jones+ 2008

Fig. 4.—Chandra HRC gray-scale images from 2006 February, with radio contours overlaid. (rms noise level of $46 \mu\text{Jy beam}^{-1}$). All images have been restored with the same beam size of 0.49×0.49 arcsec (bottom right corner of each image). There is no evidence for any X-ray extension along the jet direction in any case. The X-ray core gets brighter over the course of the last three observations.

SS433

Tudose et al. (2009) have observed the X-ray binary SS 433 on November 6, 2008 between 13:48-18:35 UT at 5 GHz with the European VLBI Network (EVN) using the **e-VLBI** technique. The radio telescopes participating in the experiment were: Medicina, Onsala 25m, Torun, Jodrell Bank MkII and Cambridge.

The X-ray binary SS 433 is in outburst.

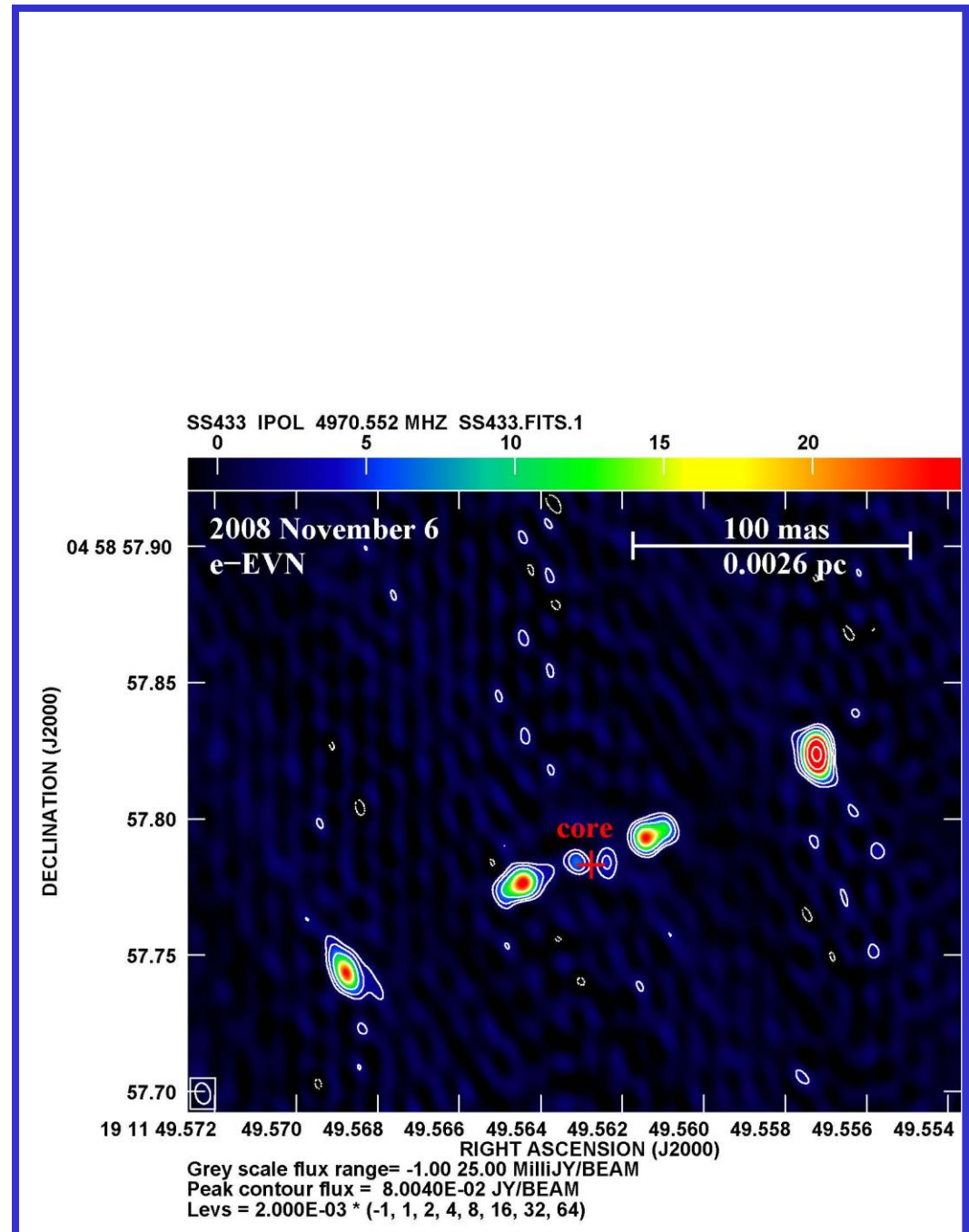


Table 1 Sources of Relativistic Jets in the Galaxy⁽¹⁾

Source	Compact object	$V_{app}^{(2)}$	$V_{int}^{(3)}$	$\Theta^{(4)}$	
GRS 1915+105	black hole	1.2c-1.7c	0.92c-0.98c	66°-70°	Transient
GRO J1655-40	black hole	1.1c	0.92c	72°-85°	
XTE J1748-288	black hole	0.9c-1.5c	>0.9c		=
SS 433	neutron star ?	0.26c	0.26c	79°	
Cygnus X-3	neutron star ?	~0.3c	~0.3c	>70°	=
CI Cam	neutron star ?	~0.15c	~0.15c	>70°	=
Circinus X-1	neutron star	≥0.1c	≥0.1c	>70°	Persistent
1E1740.7-2942	black hole				
GRS 1758-258	black hole				=
Sgr A*	black hole				=

(1) Sources reported as of December 1998.

(2) V_{app} is the apparent speed of the highest velocity component of the ejecta.

(3) V_{int} is the intrinsic velocity of the ejecta.

(4) Θ is the angle between the direction of motion of the ejecta with the line of sight.

Persistent in X => in radio: weak structures with extension on parsec scale, not variable

Transient in X => in radio: outburst/ejection events

(**BH** have $v \sim 0.9$, **NS** v smaller, v could be used to discriminate between **BH** and **NS**)

Superluminal motions (1)

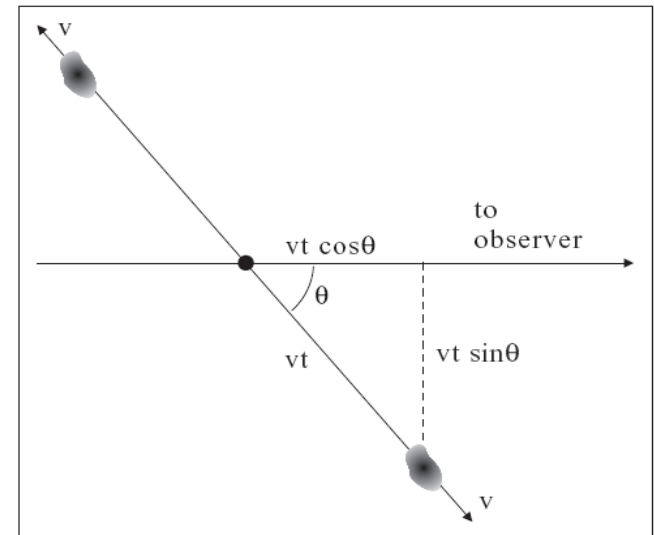
- Simoultaneous symmetric emission of two condensations with relativistic velocity, and an angle with respect the l.o.s. $\theta(0^\circ < \theta < 90^\circ)$ (Rees 1966).
- Due to the relativistic motion the approaching component appears faster and brighter than the receding component.
- Proper motions:

$$\beta = v/c$$

$$\text{a) } \mu_{app} = \frac{\beta \sin \theta}{(1 - \beta \cos \theta)} \frac{c}{D} \quad \text{approaching}$$

$$\text{b) } \mu_{rec} = \frac{\beta \sin \theta}{(1 + \beta \cos \theta)} \frac{c}{D} \quad \text{receding}$$

$D =$ source distance



Note: jets are defined as collimated emissions with aperture angle less than $<15 \text{ deg.}$ ₁₆
 (Bridle & Perley 1994 for extragalactic jets)

Superluminal motions (2)

Observed the proper motions of the approaching and the receding components (a) and (b) and multiplying them:

$$D_{\max} = \frac{c}{\sqrt{\mu_{\text{app}} \mu_{\text{rec}}}} \quad \text{Maximum distance of the source}$$
$$v_{\min} = \frac{\mu_{\text{app}} - \mu_{\text{rec}}}{\mu_{\text{app}} + \mu_{\text{rec}}} c \quad \text{Minimum velocity of the components}$$

i.e. $\beta = 1$ $\sin \theta = 1$

f.e. GRS 1915+105:

$$\mu_a = 17.6 \pm 0.4 \text{ mas/day}$$

$$\mu_b = 9.0 \pm 0.1 \text{ mas/day}$$

 $D \leq 13.7 \text{ kpc} \Rightarrow \text{Galactic source}$

Superluminal Motions (3)

- *Doppler boosting:*

$$\frac{S_{app}}{S_{rec}} = \left(\frac{1 + \beta \cos \theta}{1 - \beta \cos \theta} \right)^{k-\alpha}$$

Ratio between the flux densities of the two components

α radio spectral index

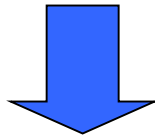
k geometrical factor

= 2 (stationary flux, continuous jet)

= 3 (discrete emission)

Multifrequency observations of GRS 1915+105

- X/gamma, Radio, mm, IR observations
- *Variabile* emission in X, Radio, IR.
- Similar characteristics in the various bands: X and radio-IR properties are correlated.



Observational evidence: connection between jet and disk

Model for GRS 1915+105 applicable to other micro-QSO
and possibly to AGN

Radio observations: variability and relativistic jets

Radio counterpart of GRS 1915+105: faint radio source with $S = 5 - 15$ mJy at 20 cm (VLA, Mirabel 1993; 1994; Mirabel & Rodriguez 1994).

- Strongly variable, with high luminosity peaks: $\max S > 1$ Jy at 20 cm

- First galactic source with superluminal motions: march 1994
 \Rightarrow double jets with relativistic motion in opposite directions with respect to the variable core

Apparent velocity of the clouds in the plane of sky:

True velocity of the clouds: $v = 0.95c$

$$\begin{cases} v_{\text{app}}: 1.25c \\ v_{\text{rec}}: 0.65c \end{cases}$$

Angle with respect to the l.o.s: $\theta = 70^\circ$

Synchrotron emission

$d_{\max} [kpc]^*$	v_{\min}^*	S_{app} / S_{rec}^*	k^*	$P_{ej} [erg]$	$P_{jet} [erg / s]$	Γ_{bulk}
≤ 13.6	0.3-0.4c	7-9	1.3-2.3	3×10^{46}	$> 10^{38}$	2-30

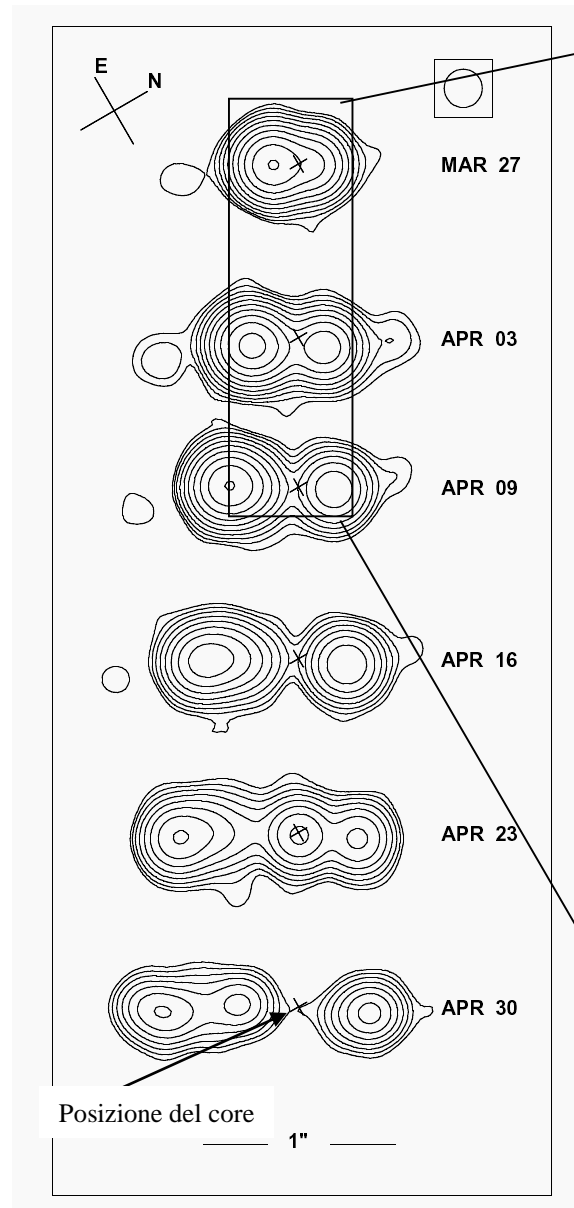
*

From model

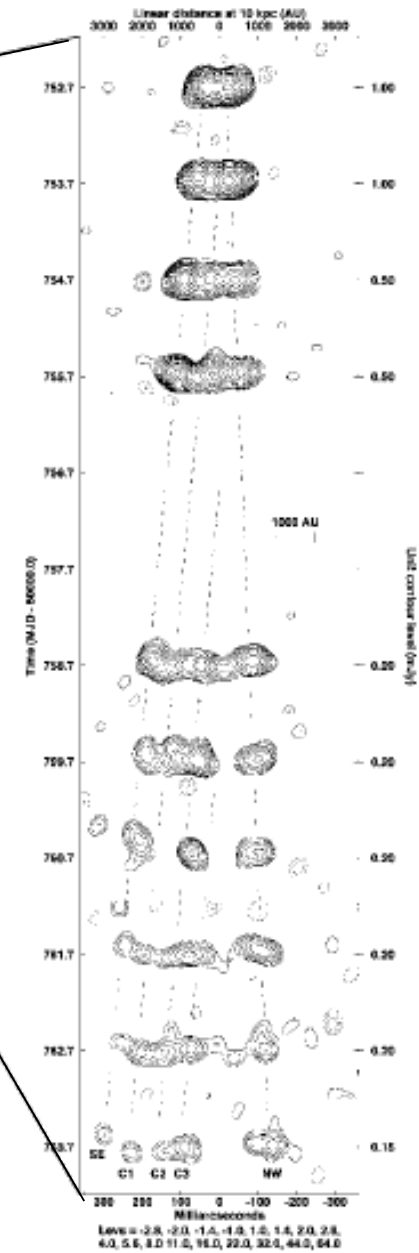
true bulk motions

Powerful jets

GRS1915+105



VLA, 3.5 cm. Maximum events in about 1 month (1994)



MERLIN, higher resolution.
Period of about 12 days

- Monitoring with radiotelescopes: GBT, VLA, MERLIN, VLBI/EVN, VLBA
- Several events have been observed (**Outburst rate** ~ 1.3 /yr)
- Two states of radio emission (Foster, 1999):

flaring: optical thin radio spectrum

relativistic emission

plateaux: flat phases in the radio light curve

optical thick radio spectrum

IR Observations of 1915+015

- IR counterpart: variable source in J, H, K bands (1.2, 1.6, 2.2 micro-m) => NIR. (Mirabel 1993, 1994)
- High resolution photometry in K band: amplitudes of oscillations, period and shape similar to the radio oscillations => NIR *synchrotron* emission (Fender 1997)
- Observations at 4-18 micro-m (ISO) => flat spectrum: synchrotron or free-free
- Simultaneous observations Radio/IR/X (Fender 1999) => light curve

Binary system with a K or M star (Grainer, 2001)

BH mass is $14 \pm 4 M_{\text{sol}}$ (the more massive stellar BH)

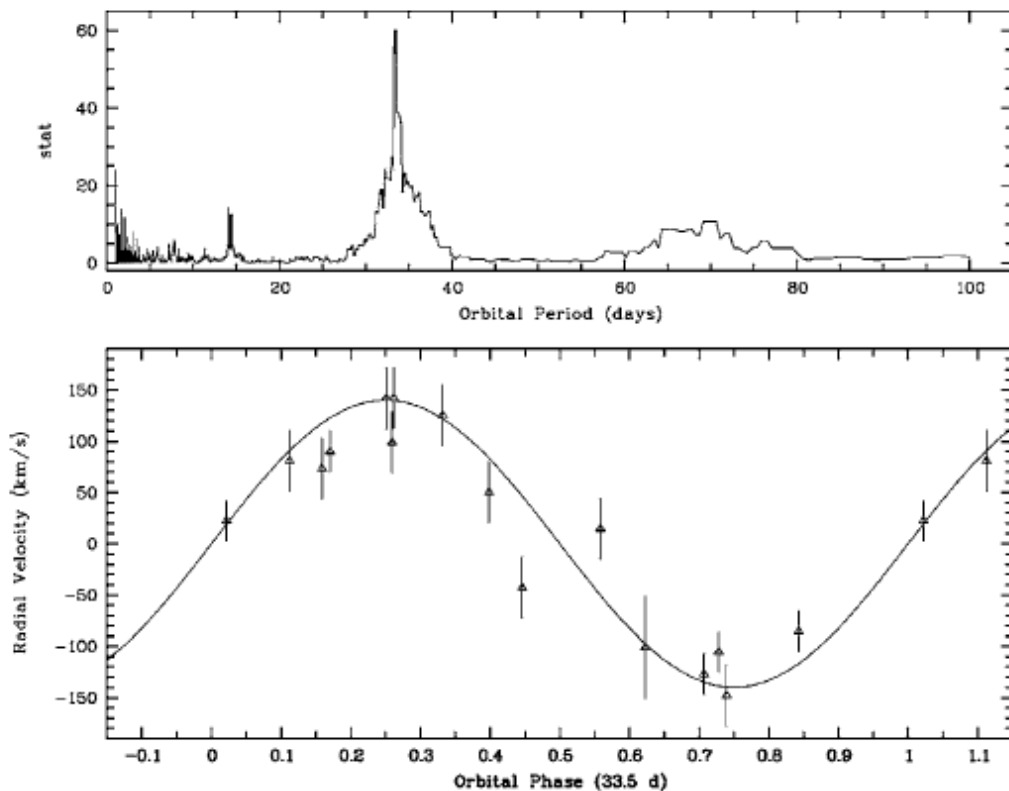


Figure 24 Orbital parameters of GRS 1915+105 from IR spectroscopy (Greiner et al. 2001a). The top panel shows the most likely orbital period, of 33.5 days, for the binary. The lower panel shows the radial velocity data folded on this orbital period. From these data a mass function—corresponding to an absolute lower limit on the mass of the accreting object—of $9.5 \pm 3.0 M_{\odot}$ can be derived. Assuming a companion mass of $\sim 1.2 M_{\odot}$ and an orbital inclination equal to the angle the jets make with the line of sight, i.e., $\sim 70^{\circ}$, then Greiner et al. estimate a mass of $14 \pm 4 M_{\odot}$ for the black hole.

Radio Oscillations

- Observed at 15 GHz; quasi sinusoidal with amplitude of ~ 50 mJy and periods from minutes to hours
- Correlate con X-ray *dips* osservati da RXTE (**Rossi X-ray Timing Explorer**) nello stesso tempo, con periodi di ricorrenza simili. (**Pooley & Fender, 1997**).

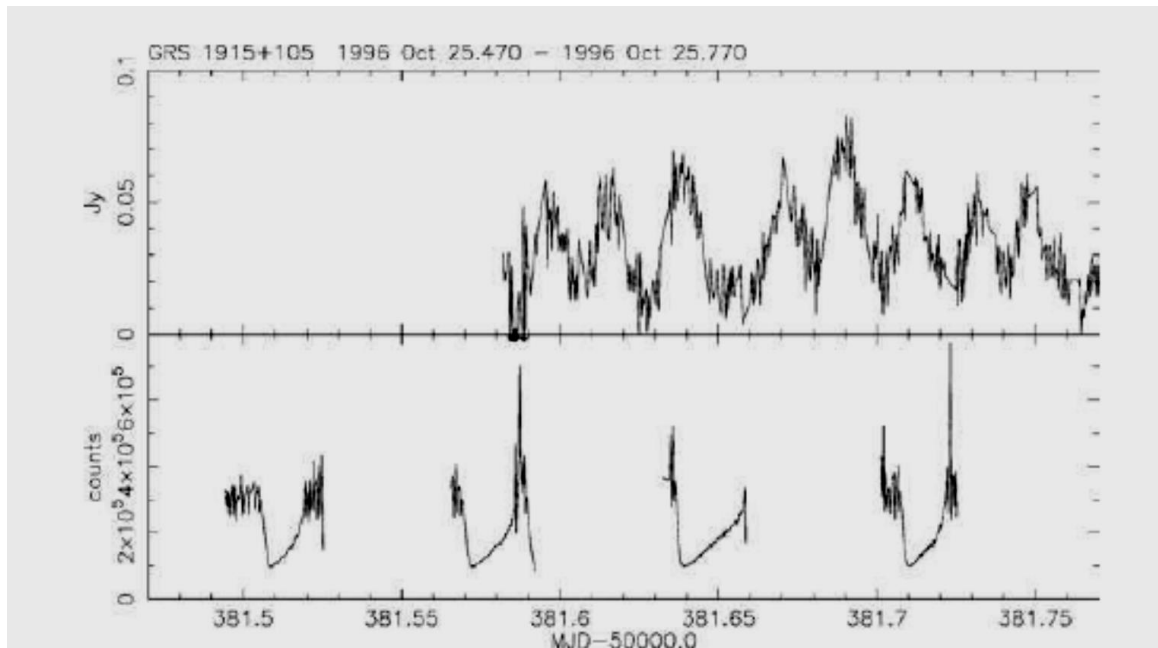


Figure 21 Simultaneous radio and X-ray observations of GRS 1915+105 in 1996, from Pooley & Fender (1997). Despite the patchy X-ray coverage there is a clear hint of an association between the semiregular X-ray dipping behavior and the radio oscillations.

Superluminal jets during the plateau phase in X

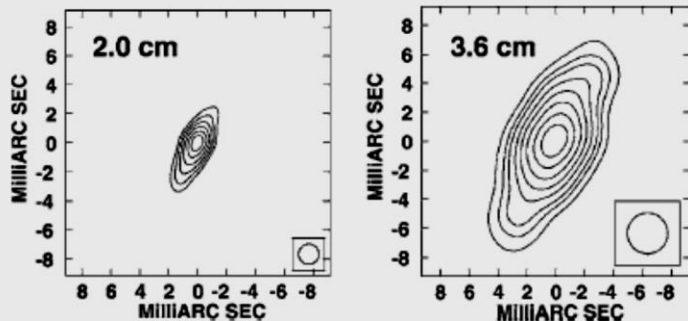


Figure 20 Compact core jet associated with the plateau—steady, hard X-ray and radio emission—state in GRS 1915+105 in April 2003 (adapted from Fuchs et al. 2003b). A similar jet in a plateau state in 1998 was reported by Dhawan et al. (2000).

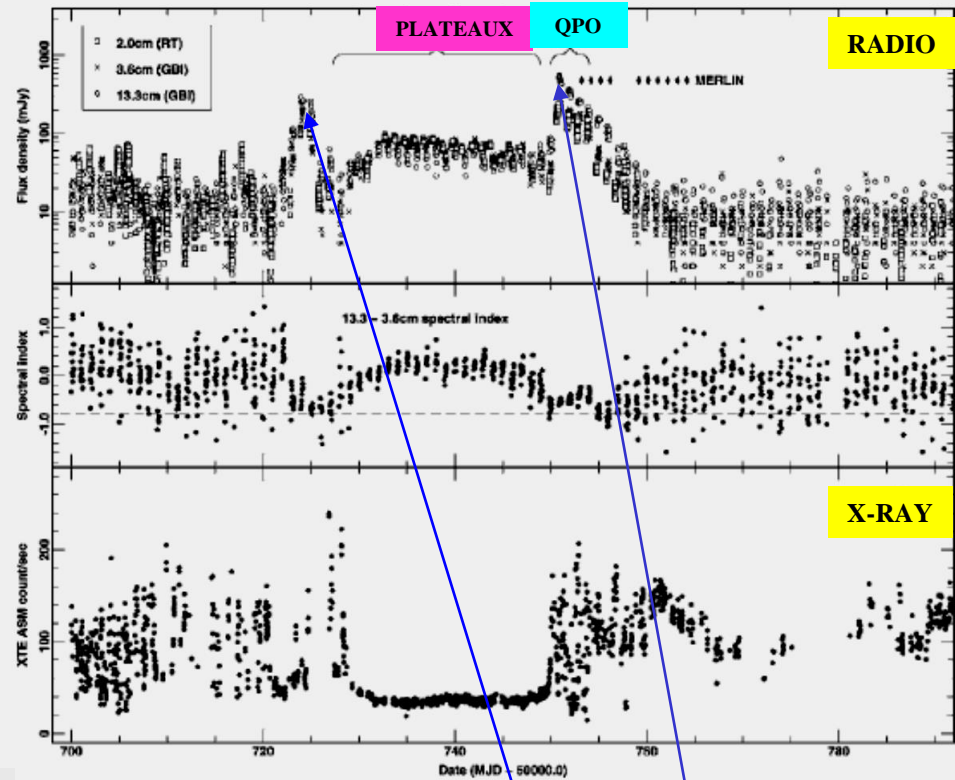
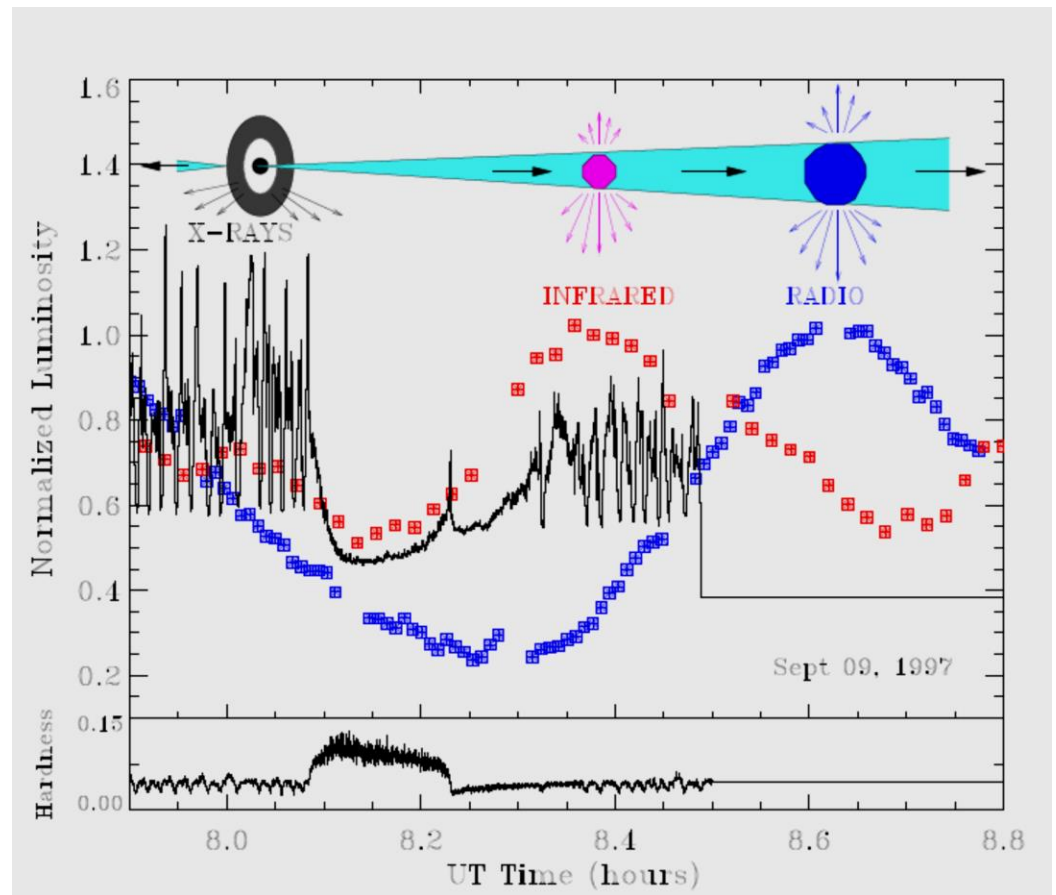


Figure 19 A plateau state in GRS 1915+105 from Fender et al. (1999). The top panel shows radio monitoring at three frequencies, from the Green Bank Interferometer (GBI) and Ryle Telescope (RT). The plateau phase lasts from approximately MJD 50730 to MJD 50750, and is associated with a flat radio spectrum (middle panel). The plateau is associated with steady X-ray emission (lower panel), which has a hard spectrum (state C). Prior to the plateau is a small, medium-strength, optically thin flare (preplateau flare in Klein-Wolt et al. 2002), and following the plateau is a larger optically thin flare (postplateau flare), which in this case was directly resolved into a relativistic ejection event (tickmarks indicate the epochs of the MERLIN observations presented in the right panel of Figure 18). Following the first postplateau flare was a period of four days of X-ray dip/radio oscillation cycles, indicated as QPO. Other occasions of plateaux have resolved the flat-spectrum radio emission into a steady jet such as those presented in Figure 20.

Quasi-periodic oscillations (QPO) in the X spectrum may be related with fundamental parameters of BH (mass, spin).



HXR dip → accretion disk

IR flare → region near to the jet base

Radio flare → jet

From multi-frequency observations:

- Jets appear after the decrease of X emission
- Jets during the phase of disk accretion replenishment
- Jet emission is not instantaneous, up to ~ 10 years
- Delay between the flare at 2 micro-m, 2 cm, 3.6 cm, 6 cm and 21 cm is consistent with the adiabatic expansion model of a cloud (proposed for AGN). The flare appears in the near-IR ($\sim 10^{-3}$ s after the emission) then in radio domain.

Parameters and assumptions used for extragalactic objects (Pacholczyk, 1970) in the 1994 outburst of GRS1915+105:

$$H \sim 50mG$$

$$W_{el} \sim 10^{43} \text{ erg}$$

Considering the duration ≤ 3 days the minimum emitting power is:

$$\sim 5 \times 10^{38} \text{ erg / s}$$

MicroQSO versus SMBH systems (AGN)

The physics of the disk-jet in the XRBs can be applied to AGN. Time scale of the processes depends on the BH mass.

- Jets in GRS 1915+105 during the plateaux

$L_{radio} \propto L_X^{0.7}$, (Gallo 2003) general relation valid for XRB; similar relation for AGN (Merloni 2003).

⇒ Stationary jets in XRBs comparable with the jets in AGN

⇒ evidence of extinction of radio emission in AGN in the interval

L_X / L_{edd} corresponding to the extinction of the jet in the soft states of XRBs. (Maccarone 2003)

- Cycle HXdip/Rflare in AGN 3C 120 similar to that in GRS 1915+105, with 1 dip/yr, connected with SL motions.

$$10^5 < \frac{M_{3C210}}{M_{GRS1915+105}} < 10^6 \quad \begin{array}{l} 1 \text{ yr (3C120)} \\ \Rightarrow \text{sec-min (GRS1915+105) OBSERVED} \end{array}$$

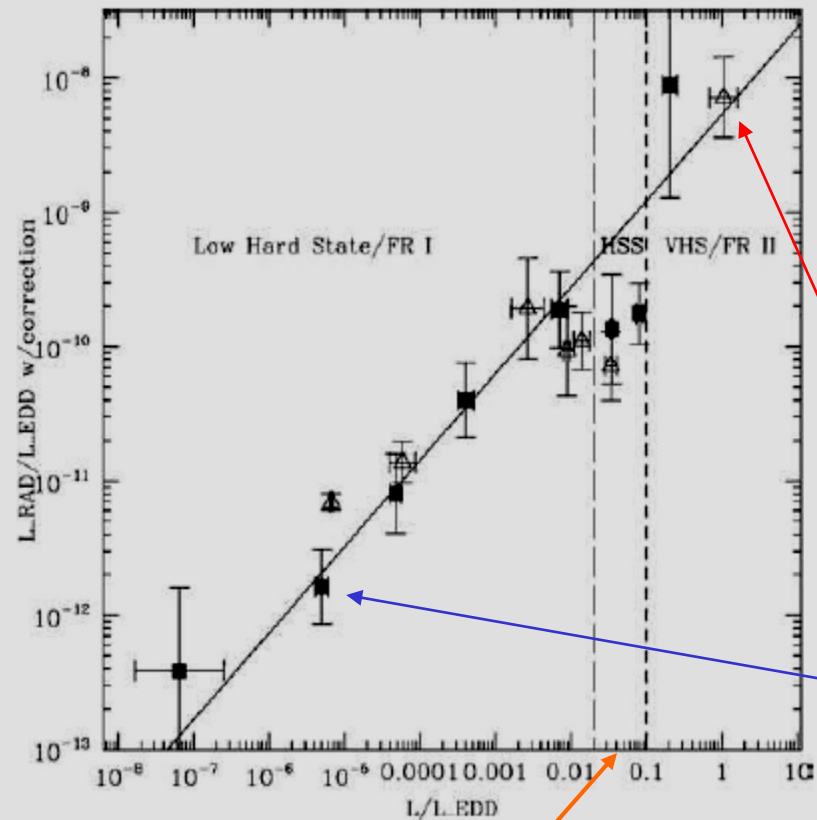


Figure 25 Jet power as a function of Eddington-scaled luminosity for X-ray binaries (*open triangles*) and AGN (*solid squares*), adjusted for the mass term of Merloni, Heinz & di Matteo (2003); from Maccarone, Gallo & Fender (2003). The reduction in radio power in the approximate range 1%–10% Eddington is well-known in X-ray binaries as the quenching of the jet in soft X-ray states, a phenomenon that may also therefore occur in AGN. The data for GRS 1915+105 lie in the most luminous bin, corresponding to FR II-type AGN.

Connection between disk and jet observed in 3C279 and 3C390.